

Effect of Annealing Temperature on Structural and Optical properties of Mn doped SnO₂ Thin Films Prepared by Sol-Gel Technique

Sunaina¹, Parikshit Sharma² and Prianka Sharma^{3*}

^{1,2,3} Department of Physics, School of Basic and Applied Sciences, Maharaja Agrasen University, Solan, INDIA

*Corresponding author Email: royprianka04@gmail.com

Available online at: www.isroset.org

Received: 04/Feb/2019, Accepted: 22/Feb/2019, Online: 30/Apr/2019

Abstract: Mn doped SnO₂ thin films were prepared by sol-gel dip coating technique. The deposited films on glass substrate were annealed at 300°C, 400°C and 500°C. The effect of annealing temperature on the structure and optical properties of the Mn-SnO₂ thin films have been studied by X-ray diffraction and UV-Vis spectrophotometry. X-ray diffraction studies shows the tetragonal rutile structure of SnO₂ with no additional phases of SnO₂. Various parameters like crystallite size, lattice constants, dislocation density and microstrain have been calculated and found to vary with annealing temperature. The optical transmission spectra shows a red shift in the position of absorption edge towards higher wavelength for Mn-doped thin films but as the annealing temperature increases, the absorption edge shifts toward lower wavelengths. The optical constants and the optical parameters were determined by the spectral transmittance data.

Keywords: Diluted Magnetic Semiconductors, Mn-SnO₂ thin films, Sol-Gel Dip Coating method, Annealing Temperature, Band Gap, Urbach's Energy.

I. Introduction

Recently, ferromagnetic and semiconducting property tuned in a single material has posed a challenging task for the experimentalists. Diluted magnetic semiconductors (DMS) have attracted importance since their property of spin degree of freedom and charge carrier can be utilized for application and fabrication of multifunctional devices. Hence, a novel physics exhibited by DMS materials, due to these intermediate interactions are expected to play a major role in material science and future spintronics [1]. The control of spin dependant phenomena in conventional semiconductors may lead to devices such as spin light-emitting diodes (spin-LEDs), spin field-effect transistors (spin-FETs) etc. [2]. There are wide variety of DMS materials like ZnO, NiO₂, TiO₂, SnO₂ etc. Among all, SnO₂ has attracted special attention because of its application in many spintronic devices due to its high Curie temperature [3]. Particular doping in SnO₂ thin films can be utilized for both *p*-type and *n*-type semiconductors. Hence, high electrical conductivity, high chemical (thermal) stability, high transmittance at near IR and visible wavelengths of SnO₂ thin films can be useful for functionalizing of various devices like transparent conductive electrodes, gas sensors, solar cell and flat panel displays [4-6]. Wide band gap property of SnO₂ thin films [7], its visible light transparency and combination with electrically low resistance region [8] can be tuned for its application in many optoelectronic devices.

Doping has always proved to be an impressive technique in controlling the electronic, spintronic and optical properties of semiconductors [9,10]. This approach brings about structural and compositional alterations in semiconductors by changing their particle or grain size. Alteration in the physical properties of SnO₂ semiconductors, by addition of new functionalities due to transition metal doping has been an attractive approach in their recent applications. Optoelectronic properties like band gap and photoluminescence and ferromagnetic ordering can be tuned by impurity doping in SnO₂ [11,12]. Transition metal doping of SnO₂ with Fe, Co, Cr [13-18] etc. have been widely reported. Recently manganese (Mn) doping [19] has been much emphasized due to its large equilibrium solubility and nearly same ionic radii as compared to Sn⁴⁺ ion for substitution. This has stimulated great interest in the optical properties SnO₂:Mn thin films since its band gap can be modified [20-23].

Till date, major concern of studies has remained on the incorporation of Mn ions of different concentration into the SnO₂ lattice. However, not much work has been done on the study of influence of annealing temperature on the structural and optical properties of Sn_{1-x}Mn_xO₂ thin films. Synthesis techniques have strong influence on the properties of Sn_{1-x}Mn_xO₂ thin films. Sol-gel process is advantageous as compared to other techniques because of low processing temperature and possibility of tailoring the starting solutions

resulting in better composition and better control of the final structure. In the present study, Mn-doped SnO₂ thin films have been fabricated on glass substrate by sol-gel dip coating method and annealed at different temperatures to study the effect of variation of annealing temperature on their structural and optical properties.

In this paper we have analyzed the structural and optical properties of pristine and Mn doped SnO₂ thin films annealed at different temperature. For structural confirmation and particle size calculation of both pristine and SnO₂:Mn thin films, X-ray diffraction is used. To investigate the changes in optical constants and parameters, doping of Mn in SnO₂ at different annealing temperature is done.

II. Experimental Details

Sol-gel dip coating method has been used to prepare SnO₂:Mn thin films. 0.5 mol of SnCl₂.2H₂O was dissolved in 50 ml absolute ethanol to prepare the solution. The solution was then stirred and refluxing was done at 80°C for 2 hrs. 2% of Manganese Chloride (MnCl₂. 4H₂O) was added as precursor into the solution. For homogenous mixing of the solution, this solution was refluxed for 4 hrs. at 80°C. The solution was then kept in air for 48 hrs. The clear homogenous solution was used for preparation of Sn_{1-x}Mn_xO₂ thin films by dip coating procedure. The films were then dried at 100°C. This procedure was repeated three times to get an even layer of solution on the substrate. Then the samples were annealed in a furnace at three different temperatures i.e. 300°C, 400°C and 500°C for 1 h in air for crystallization. After annealing the thin films were ready for characterization.

Characterization of the samples by X-ray diffraction (XRD) showed the formation of Sn_{1-x}Mn_xO₂ thin films prepared at different annealing temperatures i.e. 300°C, 400 °C and 500°C. The crystalline quality and the grain size of the samples were evaluated using XRD measurements. UV-Vis spectrophotometer was used to record the spectral transmittance of the films as a function of wavelength in the range 300-800 nm. The optical constants (refractive index and extinction coefficient) of the films were calculated from the experimental spectral transmittance data by using pointwise unconstrained minimization approach [24]. The optical band gap was obtained from Tauc's relation [25]. The Wemple-DiDomenico (WD) model and Urbach's relation were used in the analysis of oscillator, dispersion and Urbach's energy [26].

III. Results & Discussions

3.1 Structural Investigations

The crystal structure and phase purity of the samples have been determined by the X-ray diffraction patterns of SnO₂:Mn thin films. Fig. 1(a) shows the XRD pattern of pristine SnO₂ annealed at 300°C. Fig. 1(b), (c) & (d) shows

the XRD pattern of SnO₂:Mn thin films deposited on glass substrate and annealed at different temperatures i.e. 300°C, 400°C & 500°C. In Fig. 1(a) peaks corresponds to the (110), (101), (200), (211), (220), (002), (112) and (301) planes of the XRD pattern of SnO₂ films. The peaks corresponding to (110), (101), (200) & (211) are prominently observed in the XRD pattern of SnO₂:Mn thin films. The prominent peaks indexed on the basis of JCPDS file no. 41-1445 corresponds to the tetragonal rutile structure of SnO₂. No additional phases are observed such as orthorhombic phase of SnO₂, metallic Mn or other SnO based phases. This result shows that the tetragonal structure of SnO₂ is not affected by Mn impurities since the transition metal ions were successfully substituted at the Sn site. From the XRD patterns, it was observed that the intensities of the XRD peak of the SnO₂:Mn thin films increases as the annealing temperature increases. This shows that crystallite size decreases with introduction of Mn dopant because the growth of the crystal grains is inhibited due to the presence of Mn ions in SnO₂. With Mn doping the oxygen vacancies increases with Mn doping because of smaller ionic radius of Mn³⁺ ion (0.65 Å) in comparison to Sn⁴⁺ ion (0.69 Å). Hence, the crystallite size decreases due to disturbance in the long range crystallographic ordering. But annealing the samples at increasing temperature improves the crystallinity of the sample. At increasing annealing temperature, sharpness of the diffraction peaks intensifies and broadening of peak goes on decreasing. A broad diffraction peak indicates smaller particle size but with increase in annealing temperature, broadening decreases enhancing the particle size. As the annealing temperature increases, the lattice of SnO₂ films are modified since the Sn⁴⁺ ions are replaced by Mn³⁺ ions which increases the intensity of peaks in diffraction patterns. This leads to more disorders in the crystal lattice due to change of the interstitial sites of Sn⁴⁺ ions [27]. Though, doping with Mn in SnO₂ reduces the crystallite size but annealing at higher temperatures increases the crystallite size and hence improves the crystallinity of the material [28]. Scherrer's formula [29] has been used to determine the average crystallite size (D) using the diffraction peaks (110) and (101)

$$D = \frac{k\lambda}{\beta \cos \theta} \quad (1)$$

In this equation, $k=0.9$, λ represent the wavelength of the X-ray radiation, β is the full width at half maximum of the diffraction peak (in radians) and θ the Bragg diffraction angle at full width half maximum (FWHM) of the diffraction peak.

The tetragonal crystal structure is shown by the (101) and (211) peaks. For tetragonal system, the d -spacing (d_{hkl}) and lattice constants, ' a ' and ' c ', are calculated using the formula

$$\frac{1}{d^2} = \frac{h^2 + k^2}{a^2} + \frac{l^2}{c^2} \quad (2)$$

where 'd' is the interplanar distance, (hkl) are the miller indices and 'a' and 'c' are the lattice constants. In Table 1, we present the variation of the crystallite size (D), FWHM (β), interplanar-spacing (d_{hkl}), lattice parameters 'a' & 'c', microstrain (ϵ) and dislocation density (ρ) with variation in annealing temperature. The results of Table 1 are in accordance with the conclusions from the XRD patterns. From Table 1 it is clear that the full width half maxima (FWHM) values and peak positions in XRD patterns change with annealing. The FWHM of 2θ are related to the crystalline quality of the films. For pristine SnO₂ thin film annealed at 300°C, the FWHM value is lowest (0.0057). With Mn doping the FWHM value increases at 300°C (0.0154) drastically, indicating smaller crystallite size at 300°C. With increase in annealing temperature from 300°C to 500°C, the FWHM values decreases from 0.0154 to 0.0075. At 500°C, the film shows sharper and intense peak with a smaller FWHM indicating increase in particle size with increase in annealing temperature.

From Table 1, the d_{hkl} and lattice constants are also found to increase with increase in annealing temperature as the crystallite size increases. Due to annealing, the material is inflated in films because of ionic radius mismatch of Mn³⁺ and Sn⁴⁺. This increases the d-spacing and lattice constants.

The following relation has been used to determine the microstrain (ϵ) in films [30]:

$$\epsilon = \frac{\beta \cos \theta}{4} \quad (3)$$

β is the full width at half maximum of the diffraction peak (in radians) and θ the Bragg diffraction angle at full width half maximum (FWHM) of the diffraction peak. The dislocation density (ρ) has been evaluated from Williamson and Smallman's formula [30]:

$$\rho = \frac{n}{D_{hkl}^2} \text{lines} / m^2 \quad (4)$$

where D_{hkl} is the crystallite size calculated from Scherrer's formula and $n=1$ for minimum dislocation density. Microstrain in films can be developed by deposition conditions of impurity dopant. Presence of impurities in the reactant solution is responsible cause for lattice mismatch. As the annealing temperature increases, the Sn atoms move from interstitial sites to grain boundaries which reduces lattice mismatch due to recrystallization. As a result

microstrain and dislocation density of the film decreases. At lower annealing temperature, crystal growth is slow and particle size is small. But on annealing, growth of the particle has been observed. This may be due to coalescence phenomena responsible for reorganization of grains in the films, thus leading to densification of film occurring by filling the voids and reducing strains between grain boundaries.

Optical Investigations

Fig. 2 shows the Sn_{1-x}Mn_xO₂ thin films transmission spectra in the visible region of wavelength 300-800 nm. High transmittance spectra, more than 80%, is seen for pure SnO₂ thin films and Mn doped SnO₂ films at different annealing temperatures show low transmittance spectra. Due to lesser scattering effects, improved crystallinity and homogeneity in structure, the pure SnO₂ film showed higher trend in transmittance spectra. Whereas the Mn-doped SnO₂ thin films showed low transmittance because of increased scattering centres like defects and grain boundaries and increased roughness in surface [31]. These patterns of interference in the transmittance spectra indicate towards uniform and homogenous films.

With Mn doping the fundamental absorption edge red shifts toward high wavelength leading to band gap narrowing due to effects arising because of sp-d exchange in the films. However, the absorption edge shifted towards lower wavelengths with increase in annealing temperature, suggesting the broadening of energy band gap in the films. This shift was observed due to doping of SnO₂ nanoparticles with transition metal ions [32-34].

Pointwise unconstrained minimization technique was used to calculate the various optical constants like refractive index and extinction coefficient of the films prepared at different annealing temperatures from the experimental data of transmission spectra. Fig. 3 & 4 show the variations of optical constants, the extinction coefficient and the refractive index of Mn doped SnO₂ thin films annealed at different temperatures with the wavelength respectively. The extinction coefficient and the refractive index increases with Mn-doping. But as the annealing temperature increases, the extinction coefficient and the refractive index of the samples decreases. The decrease in the values of extinction coefficient is attributed to increase in crystallite size due to absorption and grain scattering. According to the XRD patterns as the crystallite size increases the grain boundaries decreases in SnO₂:Mn thin films leading to less light scattering. The extinction coefficient (k) has been calculated using the relation [35]:

$$k = \frac{2.303}{d} \log \frac{1-R}{T} \quad (5)$$

The change in refractive index with annealing temperature observed for SnO₂:Mn thin films results from the contribution due to lattice contraction and disorder in the films [36] correlated with the XRD results.

The transparent DMS material's refractive index plays a major role in the designing of various magneto-optical devices. The single electronic oscillator expression described by Wemple-DiDomenico gives the transparent region's dispersion [26]:

$$n^2 - 1 = \frac{E_0 E_d}{E_o^2 - E_d^2} \quad (6)$$

where E_d is the dispersion relation energy and E_o is the single oscillator energy. The parameter E_d which describes the interband optical transition depended on the chemical bonding related with the chemical valence and its coordination number. Also the optical properties of these materials are strongly affected by their atomic quantities. Thus, the variation of E_o and E_d parameters could bring about changes in material and structural arrangements along with variation in their optical constants. Since, $E_o \approx E_g$ shows relation between E_o , the oscillator energy, and E_g , the optical band gap, hence E_o and E_d parameters were calculated from the intercept $(E_o E_d)$ and slope $(E_o E_d)^{-1}$ of $(n^2 - 1)^{-1}$ vs. $(hv)^2$ plots. The E_o and E_d values are given in Table 2.

The Mn-doping decreases the value of E_o and E_d parameters. This indicates that Mn doping lowers the oscillator energy and transition strength compared to the pure SnO₂ thin films. But as the annealing temperature increases, the crystallite size increases, E_o & E_d values also increases indicating increase in the strength of transition and oscillator energy. Tauc's relation was used to determine the optical band gap, E_g , of SnO₂:Mn thin films [37]:

$$\alpha hv = A^* (hv - E_g)^{1/2} \quad (7)$$

where α is the absorption coefficient, A^* is a constant, (hv) is the photon energy and E_g is the energy band gap. The absorption coefficient (α) is calculated from the relation [36]:

$$\alpha = \frac{2.303}{d} \log \frac{1-R}{T} \quad (8)$$

The variation in $(\alpha hv)^2$ with hv is observed for the Sn_{1-x}Mn_xO₂ thin films in Fig. 5. The linear portion of plot $(\alpha hv)^2$ with (hv) is extrapolated to intercept the photon energy values to obtain the energy band gap. The $(\alpha hv)^2$ versus hv

curve gives direct optical band gap for SnO₂:Mn thin films since the plot asymptotically tend towards a linear portion. The band gap for pristine SnO₂ thin film was measured to be 3.5 eV. Thus measured band gap value is smaller than the value of bulk SnO₂ (3.6 eV) reported. The calculated E_g values are given in Table 2. The measured optical band gap increases from 2.51 eV to 3.4 eV with increase in annealing temperature as the crystallite size increases which cannot be explained with quantum confinement phenomenon normally. Since, the XRD patterns show no presence of manganese oxide phase hence the narrowing of band gap can be explained by neglecting the effect of alloying. The increase in band gap with increasing annealing temperature can be explained due to exchange interactions of sp-d valence orbitals between the localized d electrons of Mn³⁺ ion and band electrons which arise because Sn⁴⁺ ions replace these ions.

Often the band gap of semiconductor shows the formation of band tailing due to doping in the semiconductors with any kind of impurity. This leads to creation of optical band gap (E_g) due to the photons absorption as a result of transitions from edge of valence band of occupied states occurring at lower energies to the conduction band of unoccupied states. Thus, the Urbach rule was used to show the absorption behaviour at lower photon energy for Mn-doped SnO₂ thin films [37]:

$$\alpha = \alpha_o \exp\left(\frac{hv}{E_u}\right) \quad (9)$$

where α_o is a constant and E_u is the Urbach energy. The Urbach energy explains the width of the tails of localized states in the band gap. The inverse of slope of $\ln \alpha$ as a function of energy gives the E_u values. It is observed that with Mn doping, the Urbach's energy increases but as the annealing temperature increases, the Urbach's energy decreases as the crystallite size increases. This might be due to reason that with Mn doping some kind of defects like oxygen vacancies or structural disorders may appear which changes the localized states width in the optical band. These results show that optical band gap decreases with increase in the width of the tail states. However, as the annealing temperature increases, the optical band gap increases and the width of the tail states decreases.

IV. Conclusions

Pristine and Mn-doped SnO₂ thin films were annealed at different temperatures i.e. 300°C, 400°C and 500°C. The X-ray diffraction patterns show the tetragonal rutile structure of pure SnO₂. Introducing Mn dopant inhibits the growth of the crystal but annealing the samples at increasing temperature improves the crystallinity of the sample. The

transparency of the film was confirmed by the optical transmittance spectra of the films in the visible region. The optical constants (extinction coefficient and the refractive index) tend to increase with Mn –doping. But as the annealing temperature increases, the extinction coefficient and the refractive index of the samples decreases. It was observed that the dispersion parameters were according to the single oscillator model. The measured band gap was found to be 3.5 eV for pristine SnO₂ thin film. The calculated optical band gap of SnO₂:Mn thin film increases from 2.51 eV to 3.4 eV with increase in annealing temperature as the crystallite size increases which is accompanied by narrowing of the Urbach's tail.

References

- [1]. T.A. Dar, A. Agrawal, P. Sen, "Role of Ni Doping on structural, Electronic and Transport Properties of ZnO Thin Films", *International Journal of Scientific Research in Physics and Applied Sciences*. Vol. 3, pp 2348-3423, 2015.
- [2]. S.J. Pearton, W.H. Heo, M. Ivill, D.P. Norton, T. Steiner, "Dilute Magnetic Semiconducting Oxides", *Semicond.Sci. Technol.* Vol. 19, No. 59, 2004.
- [3]. Y. Xu, Y. Tang, C. Li, G. Cao, W. Ren, H. Xu, Z. Ren, "Synthesis and Room-Temperature Ferromagnetic Properties of Single-Crystalline Co-doped SnO₂ Nanocrystals Via a High Magnetic Field", *J. Alloys Compd.* Vol. 481, pp 837-840, 2009.
- [4]. S. SujathaLekshmy, G.P. Daniel, K. Joy, "Microstructure and Physical Properties of Sol-Gel Derived SnO₂: Sb Thin films for Optoelectronic Applications", *Appl. Surf. Sci.* Vol. 274, pp 95-100, 2013.
- [5]. S. SujathaLekshmy, K. Joy, "SnO₂ Thin Films Doped with Indium Prepared by Sol-Gel Method: Structure, Electrical and Photoluminescence Properties", *J. Sol-Gel Sci. Technol.* Vol. 67, pp 29-38, 2013.
- [6]. S. SujathaLekshmy, L.V. Maneeshya, P.V. Thomas, K. Joy, "Intense UV Photoluminescence Emission at Room Temperature in SnO₂ Thin Films", *Indian J. Phys.* Vol. 87, pp 33-38, 2013.
- [7]. C. Drake, S. Seal, "Band Gap Energy Modifications Observed in Trivalent In Substituted Crystalline SnO₂", *Appl. Phys. Lett.* Vol. 90, No. 233117, 2007.
- [8]. C. Kilic, A. Zunger, "Origins of Coexistence of Conducting and Transparency in SnO₂", *Phys. Rev. Lett.* Vol. 88, No. 95501, 2002.
- [9]. S.C. Erwin, L. Zu, M.I. Haftel, A.L. Efros, T.A. Kennedy D.J. Norris, "Doping Semiconductor Nanocrystals", *Nature* Vol. 436, No. 03832, pp 91-96, 2005.
- [10]. D.J. Norris, A.L. Efros, S.C. Erwin, "Doped Nanocrystals", *Science* Vol. 319, No. 5871, pp 1776-1785, 2008.
- [11]. I.J. Berlin, J.S. Lakshmi, S. SujathaLekshmy, G.P. Daniel, P.V. Thomas K. Joy, "Effect of Sol Temperature on the Structure, Morphology, Optical and Photoluminescence Properties of Nanocrystalline Zirconia Thin Films", *J. Sol-Gel Sci. Technol.* Vol. 58, pp 669-676, 2011.
- [12]. K. Joy, S. SujathaLekshmy, P.B. Nair, G.P. Daniel, "Band gap and Superior Refractive Index Tailoring Properties in Nanocomposite Thin Film Achieved through Sol-Gel Co-deposition Method", *J. Alloy. Compd.* Vol. 512, pp 149-155, 2012.
- [13]. J.M.D. Coey, A.P. Douvalis, C.B. Fitzgerald, M. Venkatesan, "Ferromagnetism in Fe-doped SnO₂ Thin Films", *Appl. Phys. Lett.* Vol. 84, pp 1332-1334, 2004.
- [14]. N.H. Hong, J. Sakai, W. Prellier, A. Hassini, "Transparent Cr-doped SnO₂ Thin Films: Ferromagnetism beyond Room Temperature with a Giant Magnetic Moment", *J. Phys. Condens. Matter* Vol. 17, pp 1697-1702, 2005.
- [15]. X.F. Liu, W.M. Gong, J. Iqbal, B. He, R.H. Yu, "Structural Defects Mediated Room Temperature Ferromagnetism in Co-doped SnO₂ Insulating Films, *Thin Solid Films*", Vol. 517, pp 6091-6095, 2009.
- [16]. M.M. Bagheri-Mohagheghi, N. Shahtahmasebi, M.R. Alinejad, A. Youssefi, M. Shokooh-Saremi, "Fe-doped SnO₂ Transparent Semiconducting Thin Films Deposited by Spray Pyrolysis Technique: Thermoelectric and p-type Conductivity Properties", *Solid State Sci* Vol. 11, pp 233-239, 2009.
- [17]. K. Galatsis, L. Cukrov, W. Wlodarski, P. McCormick, K. Kalantarzadeh, E. Comini, G. Sberveglieri, "p- and n-type Fe-doped SnO₂ Gas Sensors Fabricated by the Mechanochemical Processing Technique", *Sens. Actuators B. Chem.* Vol. 93, pp 562-565, 2003.
- [18]. M.M. Bagheri-Mohagheghi, M. Shokooh-Saremi, "The Electrical, Optical, Structural and Thermoelectrical Characterization of n- and p-type Co-doped SnO₂ Transparent Semiconducting Films Prepared by Spray Pyrolysis Technique", *Physica B* Vol. 19, pp 4205-4210, 2010.
- [19]. A. Kaushal, P. Bansal, R. Vishnoi, N. Choudhary, D. Kaur, "Room Temperature Ferromagnetism in Sn_{1-x}Mn_xO₂ Nanocrystalline Thin Films Prepared by Ultrasonic Spray Pyrolysis", *Physica B* Vol. 404, pp 3732-3738, 2009.
- [20]. F. Gu, S.F. Wang, M.K. Lu, G.J. Zhou, D. Xu and D. R. Yuan, "Photoluminescence Properties of SnO₂ Nanoparticles Synthesized by Sol-Gel Method", *J. Phys. Chem. B* Vol. 108, No. 35, pp 8119-8123, 2004.
- [21]. H. Kimuraa, T. Fukumuraa, H. Koinuma, M. Kawasaki, "Fabrication and Characterization of Mn-doped SnO₂ Thin films", *Physica E* Vol. 10, pp 265-267, 2001.
- [22]. R. Brahama, M.G. Krishna, A.K. Bhatnagar, "Optical, Structural and Electrical Properties of Mn-doped Tin Oxide Thin Films", *Bull. Mater. Sci* Vol. 29 pp 317-322, 2006.
- [23]. Y. Xiao, Sh. Ge, Li. Xi, Y. Zuo, X. Zhou, B. Zhang, L. Zhang, Ch. Li, X. Han, Zh. Wen, "Optical and Ferroelectric Properties of K_xNa_{1-x}Ba₂Nb₅O₁₅", *Appl. Surf. Sci.* Vol. 2547, pp 459-463, 2008.
- [24]. E.G. Birgin, I. Chambouleyron, J.M. Martinez, "Determination of Thickness and Optical Constants of Amorphous Silicon Films from Transmittance Data", *J. Comput. Phys.* Vol. 77, No. 2133, 2000.
- [25]. J. Tauc, "Amorphous and Liquid Semiconductor (Plenum, New York, 1974).
- [26]. M. DiDomenico, S.H. Wemple, "Oxygen-Octahedra Ferroelectrics I. Theory of Electro-Optical and Nonlinear Optical Effects", *J. Appl. Phys.* Vol. 40, pp 720-734, 1969.

- [27]. M.M. Bagheri-Mohagheri, M. Shokooh-Saremi, "Electrical, Optical and Structural Properties of Li-doped SnO₂ Transparent Conducting Films Deposited by the Spray-Pyrolysis Technique: A Carrier-Type Conversion Study", *Semicond. Sci. Technol.* Vol. 19 No. 6, pp 764-769, 2004.
- [28]. Z.M. Tian, S.L. Yuan, J.H. He, P. Li, S.Q. Zhang, C.H. Wang, Y.Q. Wang, S.Y. Yin, L. Liu, "Structural and Magnetic Properties in Mn Doped SnO₂ Nanoparticles Synthesized by Chemical Co-Precipitation Method", *J. Alloys Compd.* Vol. 466, No.1, pp 26-30, 2008.
- [29]. B.D. Cullity, S.R. Stock, *Elements of X-Ray Diffraction*, 3rd Edn. Prentice Hall, Upper Saddle River (2001) 388.
- [30]. S. Prabhakar, M. Dhanam, "CdS Thin Films from Two Different Chemical Baths- Structural and Optical Analysis", *J. Cryst. Growth* Vol. 285, pp 41-48, 2005.
- [31]. F.E. Ghodsi, J. Mazloom, "Optical, Electrical and Morphological Properties of p-type Mn-doped SnO₂ Nanostructured Thin Films Prepared by Sol-Gel Process", *Appl. Phys. A* 108 (2012) 693-700.
- [32]. Sathyaseelan, K. Senthilnathan, T. Alagesan, R. Jayavel, K. Sivakumar, "Formation of Mn doped SnO₂ Nanoparticles Via the Microwave Technique: Structural, Optical and Electrical Properties", *Mater. Chem. Phys.* Vol. 124, pp 1046-1050, 2010.
- [33]. A. Bouaine, N. Brihi, G. Schmerber, C. Uihag-Bouillet, S. Colis, A. Dinia, "Structural, Optical and Magnetic Properties of Co-doped SnO₂ Powders Synthesized by the Coprecipitation Technique", *J.Phys. Chem. C* Vol. 111, pp 2924-2928, 2007.
- [34]. T.N. Soitah, C. Yang, L. Sun, "Structural, Optical and Electrical Properties of Fe-doped SnO₂ Fabricated by Sol-Gel Dip Coating Technique", *Mater. Sci. Semicond. Process*, Vol. 13, pp 125-131, 2010.
- [35]. M.M. Abd El. Raheem, "Optical Properties of GeSeTI Thin Films", *J. Phys.: Condens. Matter* Vol. 19, No. 216209, 2007.
- [36]. L. Wang, L. Meng, V. Teixeira, S. Song, Z. Xu, X. Xu, "Structural and Optical Properties of ZnO: V Thin Films with Different Doping Concentrations", *Thin Solid Films* Vol. 517, pp 3721-3725, 2009.
- [37]. D.L. Wood, J. Tauc, "Weak Absorption Tails in Amorphous Semiconductors", *Phys. Rev. B* Vol. 5, pp 3144-51, 1972.

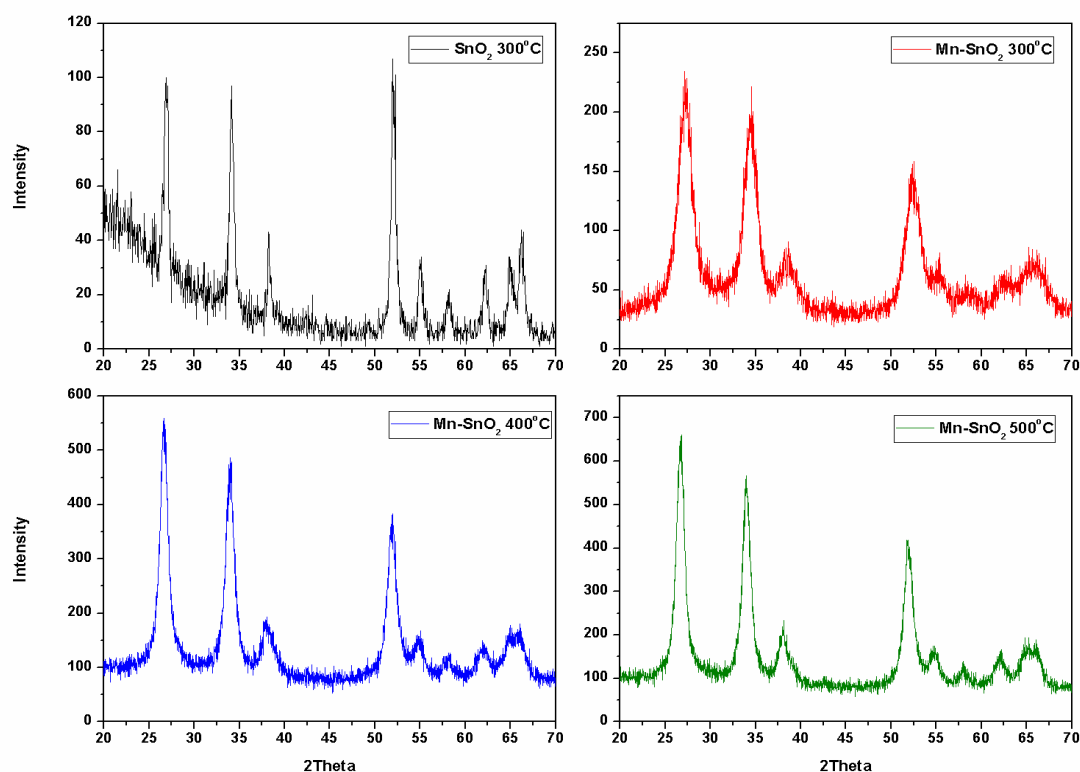


Fig. 1 XRD patterns of Mn-doped SnO₂ thin films at different annealing temperatures (a) pristine SnO₂ at 300°C (b) Mn-SnO₂-300°C (c) Mn-SnO₂-400°C (d) Mn-SnO₂-500 °C.

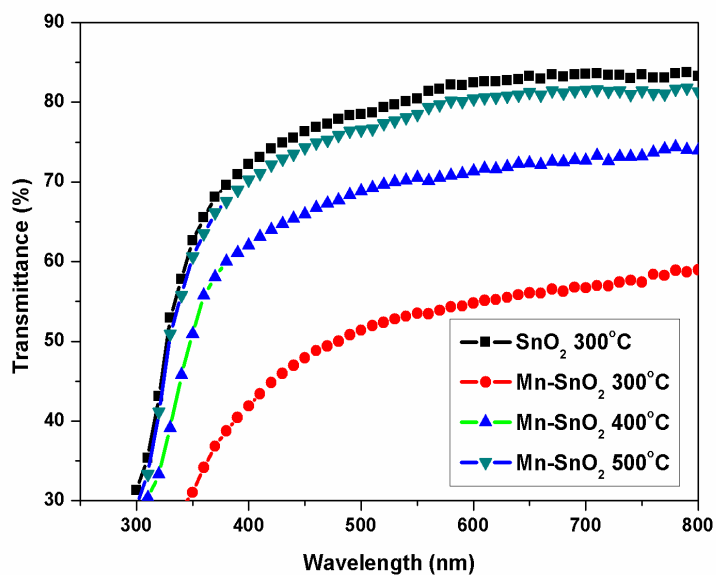


Fig. 2 Transmission spectra of pristine SnO₂ at 300°C and Mn-doped SnO₂ thin films at different annealing temperatures 300°C, 400°C & 500°C.

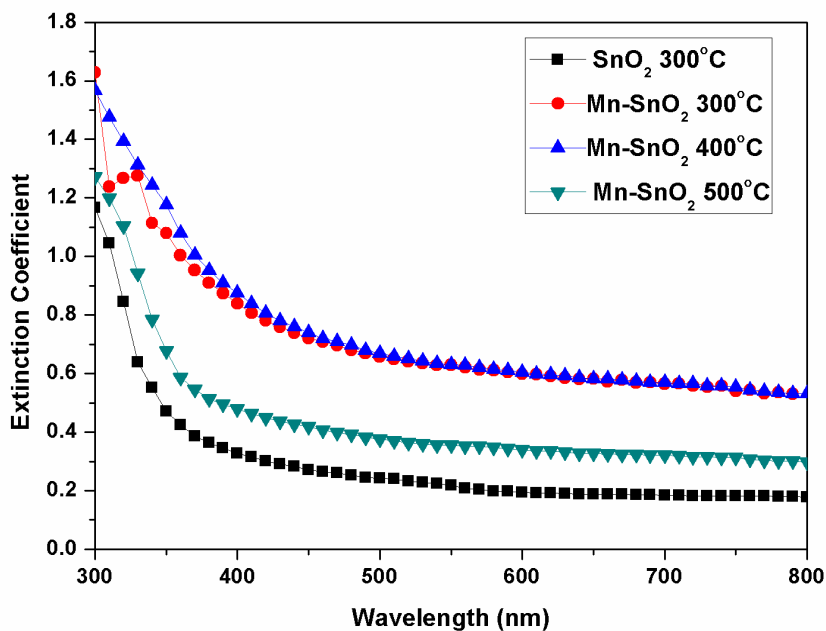


Fig. 3 Variation of Extinction Coefficient of pristine SnO₂ at 300°C and Mn-doped SnO₂ thin films at different annealing temperatures 300°C, 400°C & 500°C with wavelength.

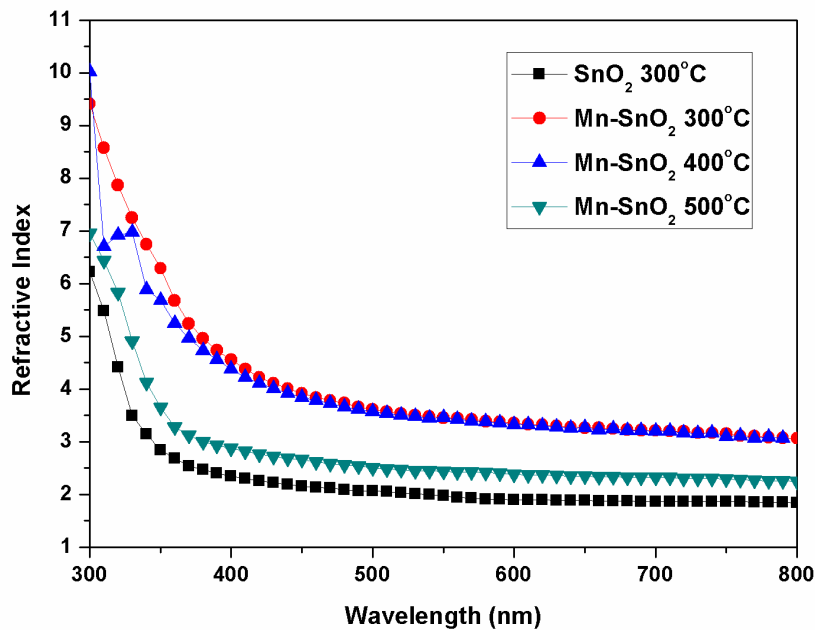


Fig. 4 Variation of Refractive Index of pristine SnO₂ at 300°C and Mn-doped SnO₂ thin films at different annealing temperatures 300°C, 400°C & 500°C with wavelength.

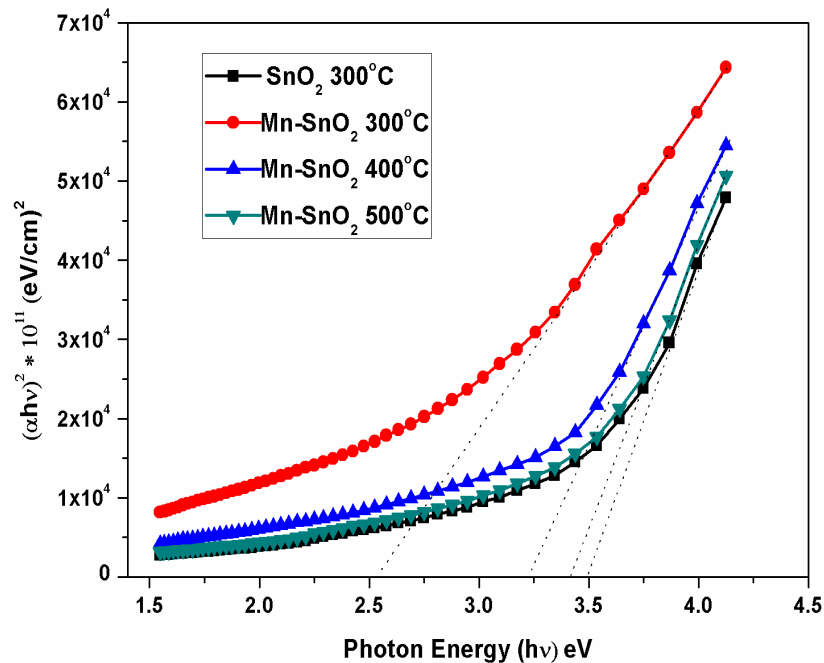


Fig 5 The plot of $(\alpha h\nu)^2$ vs. photon energy of pristine SnO₂ at 300°C and Mn-doped SnO₂ thin films at different annealing temperatures 300°C, 400°C & 500°C.

TABLE 1 Structural parameters of the Mn-doped SnO₂ thin films at different annealing temperatures.

| Sample Name | Crystallite Size (nm) | FWHM | d_{hkl} (°Å) | Lattice Constants | | ϵ (*10 ⁻³) | ρ (*10 ¹⁵) |
|--------------------------|-----------------------|--------|----------------|-------------------|--------|---------------------------------|-----------------------------|
| | | | | a (°Å) | c (°Å) | | |
| SnO ₂ -300 | 25.2 | 0.0057 | 2.64 | 4.72 | 3.18 | 1.3 | 1.5 |
| Mn-SnO ₂ -300 | 9.3 | 0.0154 | 2.54 | 4.68 | 3.04 | 3.7 | 11.5 |
| Mn-SnO ₂ -400 | 11.26 | 0.0127 | 2.62 | 4.69 | 3.16 | 3.0 | 7.8 |
| Mn-SnO ₂ -500 | 19.25 | 0.0075 | 2.63 | 4.70 | 3.17 | 1.8 | 2.6 |

TABLE 2 Variation of direct optical band gap (E_g), Urbach energy (E_u), single oscillator energy (E_o), dispersion energy (E_d) of Mn-doped SnO₂ at different annealing temperatures.

| Sample | E _g (eV) | E _u (meV) | E _o (eV) | E _d (eV) |
|--------------------------|---------------------|----------------------|---------------------|---------------------|
| SnO ₂ -300 | 3.5 | 164 | 4.06 | 4.86 |
| Mn-SnO ₂ -300 | 2.51 | 271 | 2.6 | 1.27 |
| Mn-SnO ₂ -400 | 3.24 | 251 | 3.06 | 4.05 |
| Mn-SnO ₂ -500 | 3.40 | 210 | 3.13 | 4.14 |